POD: Colour detection of people and objects for multi-camera video tracking

Mathew Price, Fred Nicolls, Gerhard de Jager

Department of Electrical Engineering
University of Cape Town
Rondebosch 7701, South Africa
mathew@dip.ee.uct.ac.za

Abstract

Visual tracking of humans has proved to be an extremely challenging task for computer vision systems. Often the colour appearance of a person can provide enough information to identify an object or person in the short-term. However, the imprecise nature of colour measurements typically encountered in image processing has limited their use. This paper presents a system which uses the colour appearances of objects and people for tracking across multiple camera views in a video surveillance network. A distributed framework for creating and sharing visual information between several cameras is suggested, including a simple method for generating relative colour constancy. Tracking has been approached from a classification standpoint allowing the system to cope with multiple occlusions, variable camera pose, and asynchronous video feeds. Results indicate that the system could be used by 3-D tracking methods to recover from failed tracking.

1. Introduction

Object tracking has drawn a large interest in Computer Vision research due to the wide range of applications it encompasses. One such application applies to the area of computer-aided surveillance. Large buildings regularly use CCTV networks to monitor the movements of people in order to provide security and safety. This leads to a bottleneck of information since an operator can only manage a finite number of camera views accurately at one time. The idea of computer-aided surveillance fits into the intermediatory role of filtering out uninteresting events and drawing the operators' attention to items of specific importance (eg. people accessing restricted areas). A basic requirement of such a system, therefore, is the ability to keep track of several people simultaneously, especially their transitions between different camera views.

One interesting problem that arises is the issue of tracker initialisation. Many predictive tracking techniques have been developed. However, a common weakness in many of these systems is their dependence on parameter initialisation. Since a prediction is based on a current assumption and a noisy observation, errors are cumulative and can lead to eventual target loss. Recovery then requires that the tracker be re-initialised to the target's current position. The framework of tracking systems often does not allow for this.

The system proposed here approaches the tracking problem from a classification standpoint. Often the colour appearance of a person can provide enough information to determine their identity and thus their position in the short-term. Therefore, by modelling this colour appearance as a set of features, colour matching can be used to build a likelihood response to the model's spatial position in an arbitrary image. This one-shot style of tracking has the advantage of being able to deal with occluding objects, movement between multiple camera views and asynchronous video feeds. In addition, the framework is extremely flexible, allowing optional integration with a variety of information such as camera pose, geometric features and motion tendencies.

2. System Overview

The primary goal of the system is to provide a suitable framework for person/object matching that can be extended over a network of cameras. Since video processing is extremely resource-hungry, a distributed computing, bottom-up paradigm was chosen as the basis for this framework.

The basic task of the system is as follows. A camera provides input frames to the Person/Object Detector (POD). Previously trained colour object models are then used in a matching process which identifies the location (if any) of the target in the input frame.

The nodes in the distributed framework, shown in Figure 1, have been defined by three primary functions: Processing; Storage; and Management. While the diagram depicts that each node be allocated its own computer, the framework is intended to be flexible so that multiple node processes can be economically run on a single machine. Naturally, this only applies if real-time operation is not a requirement (i.e. off-line analysis).

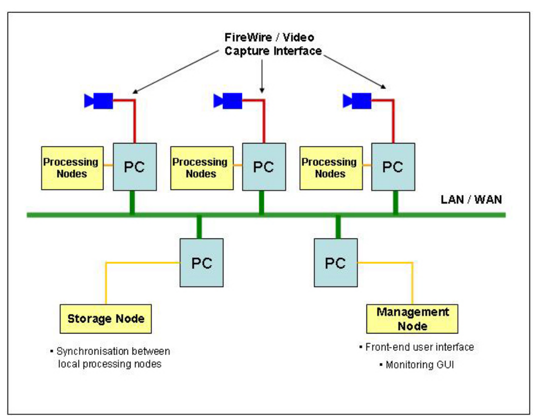

Figure 1: *Distributed Framework.*

Each processing node handles one to two cameras. They are responsible for segmentation, feature extraction, matching and model updates. High-level data, produced by the processing nodes, is then synchronised with a storage node which provides global consistency between all nodes. This framework therefore allows a modularised processing approach while preserving coherence between the multiple data streams.

2.1. Data Flow Model

The processing nodes encapsulate the entire functionality of the POD system. The system comprises several pre-processing steps which feed into the matching and training processes. A local object model repository provides the stored features of current targets which are used during matching. Figure 2 depicts these operational stages for a single processing node.

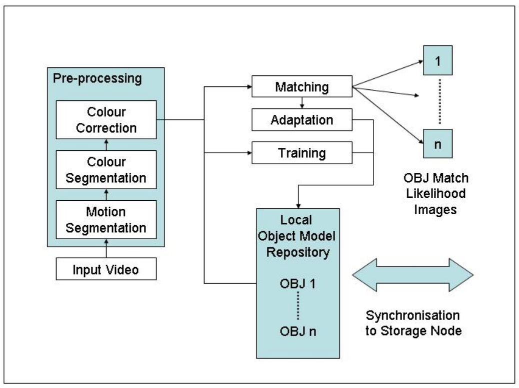

Figure 2: *Processing Node Data Flow Diagram.*

The first stage is the digital acquisition of video from a camera. The image is equalised and filtered for noise using histogram analysis and median filtering respectively.

Following this, three pre-processing steps are used to extract colour features: Motion Segmentation; Colour Segmentation; and Colour Correction. In order for the matching process to be as fast and effective as possible, it should be presented with as little irrelevant data as possible. This allows the sensitivity threshold to be increased without resulting in excess false positive matches. Searching less of the image relates directly to a faster matching process.

Motion segmentation is used to separate active people and objects from the static background, thus reducing the clutter significantly. Colour segmentation then groups similar pixel regions together, thus producing a compressed representation of the motion segmentation. This allows concise models to be constructed and greatly reduces the computational cost of matching.

When viewing an object with different cameras, it is unlikely that it will appear identical. Factors such as camera gain, shutter speed and gamma correction can contribute to large variances in image formation. Additionally, since each camera will most likely be positioned differently (probably in different rooms), environmental lighting conditions will also cause inconsistency between views. Since the system must be able to compare a person or object's colour between views, a method of calibrating all cameras to a common colour reference is necessary. Towards this end, the colour correction stage uses trained samples of a camera's response to a range of colours in order to calculate an appropriate adjustment.

The features produced by the pre-processing stages are represented by a cluster of colour centres. They are then applied to the core of the system. Initially, since the object model repository will be empty, the training stage will use the features of a specific target to discover the best representation for that target. This trained feature set is then added to the object model repository.

Once trained object models are available, the matching process is activated and produces a likelihood response to the existence of each target listed in the local repository. Close matches can be processed through an adaptation stage and used to incrementally update the stored models. This allows the system to track gradual drifts caused by lighting artifacts. Information about each matched target is compiled into a running profile and stored. Finally, the likelihood outputs can be combined, and together with the input image produce a labelled image of the position of any visible targets.

3. Pre-processing

A simple two-part segmentation scheme is used for reducing clutter and extracting colour features from objects. Firstly, *motion segmentation* by way of background subtraction removes target candidates from the static background scene. The next step involves a *colour segmentation* process whereby regions of similar colour in the foreground are grouped together and represented by a cluster of colour centres. This reduces the load on the training and matching stages, and provides a concise object description system capable of being synchronised over a network.

3.1. Motion Segmentation

Essentially, background subtraction operates by taking a frame BG containing only the static background, and subtracting a consecutive frame P from it. Any pixel difference which deviates more than a set threshold T_{diff} is considered foreground (shown in Equation 1). In this way a foreground mask M can be obtained:

$$M_{(x,y)} = \begin{cases} 1 & if\ |P_{(x,y)} - BG_{(x,y)}| > T_{diff} \\ 0 & otherwise \end{cases} \qquad (1)$$

In reality, thresholding all pixels in the image by the same amount does not provide reliable segmentation. Factors such as light distribution and colour differences can cause inconsistencies in the comparison between foreground and background pixels. An alternative to using a global threshold for the subtraction is to assume that each pixel deviates according to its own model, and thus to threshold each pixel in the context of its model [14].

Since the POD system only uses segmentation as a clutter reduction stage, either method is applicable although direct subtraction and thresholding is naturally faster.

3.2. Colour Segmentation

A batch colour segmentation method allows an efficient quantisation of the foreground into coloured components, leading to a compressed data representation which is suited to high-level processing. As colour segmentation applies to the training of object colour models, the process operates on the segmented foreground mask produced by motion segmentation.

Multiscale image processing techniques are hierarchical processes which use multiple resolutions of an image to perform analysis. These can be approached as top-down (quad-tree decomposition) or bottom-up processes (image pyramids). In the latter methods, image levels are constructed by downsampling the image by a series of filters — Gaussian in this case — which provides a smoother output.

The OpenCV library [7] provides a well optimised implementation based on the algorithm proposed in [3]. The input image (largest) can be thought of as the base of the pyramid. Each consecutive level is then built upwards, downsampling by a factor of two at each stage, until a specified maximum level is reached (commonly between 3 and 5). Two thresholds, T_1 and T_2, determine the nature of the segmentation, and linking is performed in two stages illustrated in Figure 3.

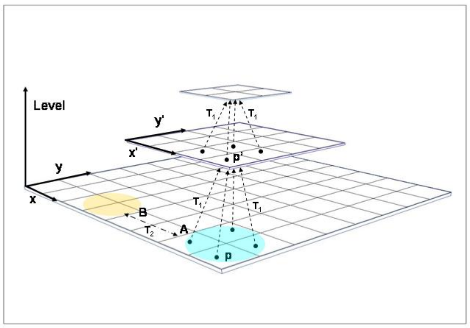

Figure 3: *Pyramid segmentation process.*

1. A link between a pixel $p_{x,y}$ on level L and its candidate father $p'_{x',y'}$ on level $L+1$ is established if: $\text{dist}(c(p_{x,y}, L), c(p'_{x',y'}, L+1)) \leq T_1$.
2. Connected components A and B are then clustered together if: $\text{dist}(c(A), c(B)) \leq T_2$.

The function $dist$ is the Euclidean distance between local property functions c for each pixel. The local property c is the type of measurement associated with a pixel, which in this case is simply the intensity of the pixel. Therefore, the distance calculated by the $dist$ function is effectively the difference in pixel intensities $|i(x,y) - i(x',y')|$.

Parameter tuning, which is dealt with in [8], was found to be fairly inconsequential. Unlike [8], the primary goal here is to reduce the mass of pixel data to a manageable number of classes (approximately 5% of the image pixels). Therefore exact parameters for maximising the quantisation are not required. In fact, a larger list of small regions which more accurately describe the original pixel colours is preferred. In general, setting $T_1 = 30$ and $T_2 = 10$ provided equitable results.

4. Colour Correction

One of the primary requirements of a multi-camera colour tracking system is consistency of colour measurements between several cameras. Colour constancy refers to the correction of colour deviations caused by a difference in illumination [17].

In light of the fact that our system is geared towards near real-time operation, it follows that a fast, robust colour constancy method is needed. Since we are using multiple cameras, the method must be insensitive to camera pose and position in addition to the usual invariants. The Video-CRM system described in [6], which has similar requirements, proposes the use of a colour calibration target. The basic idea is to show the calibration target to each camera and use the responses to calculate the gamut mapping between the two image systems.

In a large camera network it is desirable to have a more automated approach which does not encumber the users. In any case, mapping based on a target can never be totally accurate unless it takes into account colour or intensity shifts within a single image frame. This would require the calibration target to be evaluated at several positions for each view, leading to a lengthy calibration procedure.

Austermeier et al. [1] have shown a useful method for performing an unsupervised, target-based calibration scheme for normalising illumination changes. Their tests showed that a cloud of RGB pixels (plotted by omitting their spatial image placement) preserves its topology when subjected to a change in illumination. Furthermore, if the clouds of the original and resulting images are each quantised by a set of Self-Organising Map (SOM) prototypes, pixel colour can be corrected by simply translating its prototype between the two maps. SOMs have the useful feature of being able to quantise data into a set of prototypes, while at the same time preserving topological relationships between neighbouring neurons.

To clarify, usually the main usage of SOMs is for dimension reduction of feature data. However, in this application it is simply used as a 3-D data-fitting method. Another common practice is to use a 2-D neuron grid for the SOM. The main reason is because its distance matrix (depicting clustering information) is best understood in planar form. Once again, since this scheme is using the SOM's fitting ability, it is necessary to use an exact representation of the data, and thus the map is created as a 3-D lattice.

The POD colour correction module differs slightly from the implementation suggested by [1]. Modifications include: using CIELAB co-ordinates in place of RGB; using the pre-quantised colour segmentation groups rather than the entire set of input pixels; and splitting SOM training into several $(5 \times 5 \times 5)$ sets, which is more manageable.

5. Training Object Models

A primary assumption upon which the system is based is the notion that a qualitative measure for the difference between colours exists. The CIELAB colour space provides such a measure by providing uniform colour co-ordinates which describe perceptual colour differences using the magnitude of the Euclidean distance between two points. The training procedure therefore begins by converting the RGB feature list presented by the colour segmentation to their CIE L*a*b* counterparts. The system's main feature vector is therefore simply:

$$\mathbf{F}_n = (L{*}_n, a{*}_n, b{*}_n), \tag{2}$$

where $\mathbf{F}_n$ is an arbitrary feature vector. Training is split into two phases. The first is geared towards finding clusters spatially within the feature space of a presented observation set. The second clusters these cluster groups over time as additional observations are presented. The time-clustering phase therefore depends on being able to match features between between observations. This is accomplished by measuring the conditional probability $P(\mathbf{F}_n|\mathbf{C})$ of a feature $\mathbf{F}_n$ belonging to the set of centres $\mathbf{C}$ which is calculated as follows:

$$\begin{aligned} d^2_{\mathbf{F}_n\mathbf{C}_i} &= (L{*}_n - L{*}_i)^2 + (a{*}_n - a{*}_i)^2 + \\ &\quad (b{*}_n - b{*}_i)^2 \end{aligned} \tag{3}$$

$$K_{\mathbf{F}_n\mathbf{C}_i} = \frac{1}{\sqrt{2\pi\sigma_{train}^2}} e^{\left(\frac{-d^2_{\mathbf{F}_n\mathbf{C}_i}}{2\sigma^2_{train}}\right)} \quad (4)$$

$$P(\mathbf{F}_n|\mathbf{C}) = \frac{K_{\mathbf{F}_n\mathbf{C}}}{\sum_{j=1}^{m} K_{\mathbf{F}_n\mathbf{C}_j}}. \quad (5)$$

These are simply the spherical Gaussian kernel activations $K_{\mathbf{F}_n\mathbf{C}}$ normalised by the sum of activations of all current centres $\mathbf{C}_1 \ldots \mathbf{C}_m$. Since CIELAB offers uniformity, it follows that σ_{train} should be set to a constant value so that perceptual colour differences remain the same between classes. A $\sigma_{train} \approx 5$ has been found to provide good separation between colour classes.

Since similar colours will cluster uniformly in the feature space (due to the intrinsic nature of the CIELAB space), groups of like features can be represented by a Gaussian centre. Training thus involves finding the best possible group of centres which accurately quantises the input training set — i.e. a Gaussian Mixture Model.

6. Matching

Matching is divided into several stages. Each stage targets a specific interpretation of the presented data which, when combined, produces a classification likelihood of an image region for a particular object model.

The process begins by performing colour matching on the set of input features **F** produced by pyramid segmentation. This basically assigns each feature to the nearest model centres[1] in the repository **C** (a $m \times 3$ matrix). The result is a list of active model centres **X** and their centroids in image co-ordinates. Since it is likely that certain colours will match a variety of different objects, an object model confidence is constructed based on:

- Quality of the colour match
- Variety of model features matched
- Spatial density and size of the features in image space
- Consistence of area proportionality.

Simply put, an object is likely to be found in a spatial cluster in which the colour match and the variety of centres is a maximum. Furthermore, the proportional areas of the features in the cluster must be comparable to the object model's ratios. If several of these measures agree, a peak in the likelihood will appear for a certain image region. If the overall confidence exceeds a lower threshold, the object is marked as found.

6.1. Colour Matching

As with the training procedure, colour matching is done using the CIELAB distances between the extracted features **F** and object model centres **C**. Equation 6 defines the Euclidean distance for two features (as in Equation 3). **X** is then defined as the matched subset of features, which are less than $k_{match}\sigma_{match}$ Euclidean units from any of the m model centres in **C**:

$$D^2(\mathbf{F1},\mathbf{F2}) = (F1_{L*} - F2_{L*})^2 + (F1_{a*} - F2_{a*})^2 + (F1_{b*} - F2_{b*})^2 \quad (6)$$

$$\mathbf{X} = \{\mathbf{x} \in \mathbf{F} : D^2(\mathbf{x},\mathbf{C}_i) \leq (k_{match}\sigma_{match})^2, \text{ for } 1 \leq i \leq m\}. \quad (7)$$

[1]This is a one-to-many relation since several object models might claim to match a single feature.

Colour matching is thus effectively a nearest neighbour classification.

6.2. Confidence Measurement

Estimation of the confidence measurements across a 2-D image plane requires evaluation of the contribution of each matched feature for each measurement of every object class. The fact that each object feature is only represented by a central pixel dictates that a sliding window operation is needed. Unfortunately this would result in an exceptionally high computational complexity since the convolution would need to be repeated for each object class [13]. While this process can be improved using FFT fast convolution, the computational time is still proportional to the number of measurements and classes.

A less precise (yet efficient) idea is to perform measurement using a 1-D scanning algorithm which can be executed separately across the image's x and y directions. There is a possibility that a better approach might be to evaluate image quadrants [15] and use fast integral image convolution with boxlets [12]. However, separate class processing would still be required and so this alternative is left for future exploration.

Scanning proceeds by dividing the image into several evenly spaced, vertical and horizontal strips as shown in Figure 4(a). The matched features $\mathbf{X}'$ falling within a strip d_i then contribute to some property measurement $z(d_i)$ for each object model. When the measurements of all strips are concatenated, the results are two 1-dimensional likelihood signals $(\mathbf{z}_x, \mathbf{z}_y)$ spanning the width w_{im} and height h_{im} of the image respectively. Each signal is then filtered with a Gaussian kernel to smooth the disparity between the divisors (Parzen's method). Finally, the matrix multiplication of each object model's $\mathbf{z}_x$ and $\mathbf{z}_y$ vectors produces a 2-D likelihood map $\mathbf{L}_r$ for that object.

This method allows the confidence measurements to be tailored to specific areas for each image dimension. For instance, the proportionality measure holds little significance for person models in the horizontal direction since clothing divisions tend to appear vertical. As each measurement vector is one dimensional, multiple object models can be measured and stored in separate columns simultaneously. The result is an array of multi-model confidence measures created by a one-pass scan of the input image.

The following subsections describe each component of the overall confidence measurement. In order for the measurements to be combined equally, each measurement is configured to fit the range of $(0, 1)$ where 1 is the best match. Figure 4 illustrates matching for a character from a cartoon sequence.

6.3. Likelihood Map

The 2-D likelihood map $\mathbf{L}_r$ for each object r is generated by the matrix multiplication of the smoothed[2], overall confidence measurements $\mathbf{z}_x$ and $\mathbf{z}_y$ (Equation 10). These measurement vectors are constructed by the scalar multiplication of four measurement components:

$$\mathbf{z}_x = \mathbf{z}_{c_x}.\mathbf{z}_{v_x}.\mathbf{z}_{a_x}.\mathbf{z}_{p_x} \quad (8)$$

$$\mathbf{z}_y = \mathbf{z}_{c_y}.\mathbf{z}_{v_y}.\mathbf{z}_{a_y}.\mathbf{z}_{p_y} \quad (9)$$

$$\mathbf{L} = z_0(\mathbf{z}_x\mathbf{z}_y^{\mathrm{T}}), \quad (10)$$

[2]Smoothing is achieved using a Parzen window.

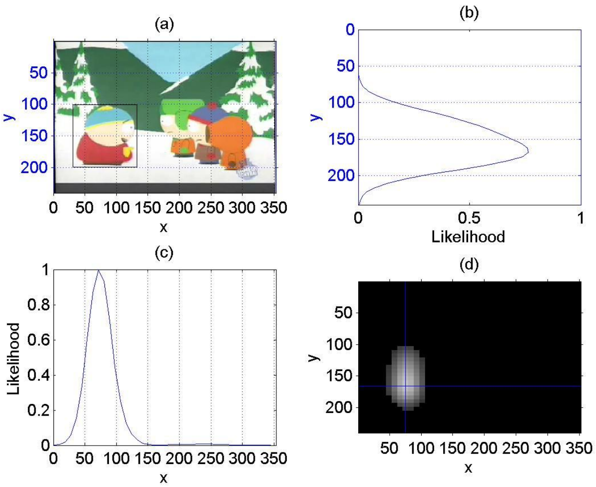

Figure 4: *Matching Example. Image (a) shows the image divisions and identifies the target (black box); Graphs (b) and (c) show the 1-D measurement signals in the y and x directions respectively; and image (d) shows the likelihood map.*

where z_0 is a scaling factor and $\mathbf{z}_c, \mathbf{z}_v, \mathbf{z}_a, \mathbf{z}_p$ are the measurement components relating to quality, variety, area and proportionality respectively. These are discussed in detail later in this section. In addition each component is the concatenated vector of the measurements for all divisions. For instance, if there are i divisions, $\mathbf{z}_{c_x}$ would consist of:

$$\mathbf{z}_{c_x} = [\mathbf{z}_{c_x}(d_1), \mathbf{z}_{c_x}(d_2), \ldots, \mathbf{z}_{c_x}(d_i)]. \tag{11}$$

Subsequently, $\mathbf{L}$ would then be an $(i \times i)$ map, similar to the example in Figure 4(d)[3].

Naturally, the number of divisions i does not have to be the same for each direction. In fact, for person tracking it can sometimes be better to allocate larger division spaces in the y direction since people are more rectangular. Note, however, that the actual division size in pixels is dependent on the size of the image dimension. Since most images are not square, this means that allocating the same number of divisions for each image dimension will not necessarily result in square likelihood regions. Generally, retaining the aspect ratio of the image is desirable, so using equal divisions for each dimension can be useful.

The effect of adjusting the number of divisions relates proportionally to the output resolution of the likelihood map. Basically, it defines the minimum detectable object size. A small value will tend to expect large objects and cause merging between object classes within close proximity. Conversely, a large division number will give a high-definition likelihood, but can cause object fragmentation.

6.4. Quality of colour match

The first measurement component quantifies the quality of the average colour match $z_c(d_i)$ between $(n \times 3)$ feature subset $\mathbf{X}'$ (the matched features falling within d_i) and its corresponding matched object model centres $\mathbf{X}'\mathbf{C}$ (i.e. $\mathbf{X}'$ and $\mathbf{X}'\mathbf{C}$ are the same size):

$$z_c(d_i) = \frac{1}{n} \sum_{j=1}^{n} e^{\left(\frac{-D^2(\mathbf{X}'_j, \mathbf{X}'\mathbf{C}_j)}{2\sigma^2_{match}} \right)}, \tag{12}$$

where D^2 is the Euclidean distance function defined in Equation 6.

6.5. Variety

If $\mathbf{X}'$ is the subset of matched features $\mathbf{X}$ falling within division d_i, then $\mathbf{h}_{d_i}(\mathbf{X}')$ is the histogram of feature areas for each object model centre in $(m \times 3)$ matrix $\mathbf{C}$ (within that division). The variety measure $z_v(d_i)$ is defined as:

$$\mathbf{v}_{d_i}(\mathbf{X}') = \begin{cases} 1 & \text{for } \mathbf{h}_{d_i}(\mathbf{X}') > h_{thresh} \\ 0 & \text{otherwise} \end{cases} \tag{13}$$

$$z_v(d_i) = \frac{1}{m} \sum_{j=1}^{m} \mathbf{v}_{d_i}(\mathbf{X}')_j. \tag{14}$$

The threshold h_{thresh} determines how many hits a bin requires before it qualifies for measurement (generally set to 1). Effectively the variety measure determines what fraction of the object model's centres is visible for each division. This relates to how much of a model is visible. A high variety will be detected where most of the object centres overlap for a particular x value.

6.6. Area Distribution

The distribution of feature areas can also hold vital information about the whereabouts of an object. Once again, $\mathbf{X}'$ is the n feature subset of $\mathbf{X}$ falling within d_i, and the area distribution $z_a(d_i)$ is:

$$z_a(d_i) = \frac{1}{A_{max}} \sum_{j=1}^{n} \text{area}(\mathbf{X}'_j), \tag{15}$$

where A_{max} is the maximum feature area throughout the image. This measurement serves to identify the division that holds the greatest area of matched pixels.

6.7. Proportionality

Proportionality refers to the ratio of the mixture of colour features for a particular object model. Often, several background regions can match a particular object's colours (seen in previous measurements), however the true object can be isolated by analysis of the proportions of these colours. The proportionality measurement is defined by the Chi-Square distance (Equation 18) between the area histograms $\mathbf{h}_{d_i}(\mathbf{X}')$ (from Equation 13) and $\mathbf{h}_{d_i}(\mathbf{C})$ (areas of object model centres) within division d_i. The histograms each have m bins which relates to the number of model centres for the specific object and are each normalised by their total sum. The Chi-Square distance provides a comparative metric between distributions and maps the interval $(-\infty, \infty)$ to $(0, 1)$ (where 0 is a close match). To make the values consistent with the other measurements (0 — no match, 1 — best match), the Chi-Square distance is subtracted from 1. Proportionality measurements $z_p(d_i)$ therefore fall within the $(0, 1)$ range where 1 is the closest possible match (Equation

[3] The likelihood map in the figure has been resized to be consistent with the image co-ordinates.

19):

$$\mathbf{h}'_{d_i}(\mathbf{X}') = \frac{\mathbf{h}_{d_i}(\mathbf{X}')}{\sum_{j=1}^{m} \mathbf{h}_{d_i}(\mathbf{X}')_j} \quad (16)$$

$$\mathbf{h}'_{d_i}(\mathbf{C}) = \frac{\mathbf{h}_{d_i}(\mathbf{C})}{\sum_{j=1}^{m} \mathbf{h}_{d_i}(\mathbf{C})_j} \quad (17)$$

$$d^2_{Chi-Square} = \sum_{j=1}^{m} \frac{(\mathbf{h}'_{d_i}(\mathbf{X}')_j - \mathbf{h}'_{d_i}(\mathbf{C})_j)^2}{\mathbf{h}'_{d_i}(\mathbf{X}')_j + \mathbf{h}'_{d_i}(\mathbf{C})_j} \quad (18)$$

$$z_p(d_i) = (1 - d^2_{Chi-Square}) \quad (19)$$

6.8. Importance Weighting

It is highly likely that multiple objects will share common colours, leading to noisy measurements. In cases where segmentation is bad, the background scene can contribute a fair amount of clutter which will cause some of the measurements to lose validity. Therefore in order to ensure that the overall confidence measurement is not compromised, each feature must be weighted by its importance.

Importance is determined based on how common a feature is found to be spatially. For instance, a colour which is visible over the entire image should be considered less important than a colour which is clustered in the vicinity of a target object when constructing each measurement.

Calculation of the importance weightings **I** involves the estimation of the spatial variance of each model centre in **C** for the entire image. This is accomplished by calculating the proportional spatial range of each feature out of the whole image. The importance weighting I_a for an arbitrary object centre $\mathbf{C}_a$ is the sum of the number of occurrences h_{sum} of $\mathbf{C}_a$ across all divisions, divided by the total number of divisions i. This is calculated for each image dimension, averaged and then squared to produce an importance value in the range $(0, 1)$[4]:

$$I_{a_x} = \frac{h_{sum_x}}{i} \quad (20)$$

$$I_{a_y} = \frac{h_{sum_y}}{i} \quad (21)$$

$$I_a = \left(\frac{I_{a_x} + I_{a_y}}{2}\right)^2 \quad (22)$$

$$\mathbf{I} = (I_1, I_2, ..., I_m), \quad (23)$$

where **I** is the vector of importance values $(I_1..I_m)$ for all object centres.

Importance weights are applied by multiplying each object centre in each measurement by its corresponding weighting. This also requires that the measurements are subsequently normalised by the sum of the object model's importance weightings in order to maintain the $(0, 1)$ measurement range.

7. Results

Acquiring meaningful results for a computer vision system is a difficult process. This arises from the fact that the exact definition of good performance varies between different types (and goals) of systems. Standard benchmarks are therefore extremely hard to come by and are generally only comparable when systems use similar test sequences.

In order to determine the overall performance and versatility of the POD system, several test sequences from different environments have been selected.

7.1. Performance Evaluation

A number of methods exist for evaluating the performance of vision systems. Even though the POD system is not entirely a stand-alone surveillance platform, it does exhibit certain similarities which warrant the use of some surveillance metrics.

7.1.1. Surveillance Metrics

The following basic metrics (taken from [2]) have been used to gauge overall system performance:

$$\text{TRDR} = \frac{\text{Total True Positives}}{\text{Total Number of Ground Truth Points}} \quad (24)$$

$$\text{FAR} = \frac{\text{Total False Positives}}{\text{Total True Positives + Total False Positives}} \quad (25)$$

$$\text{OTE} = \frac{1}{N_{rg}} \sum_{i=1}^{N_{rg}} \sqrt{\frac{(xg_i - xr_i)^2 + (yg_i - yr_i)^2}{w_{im}^2 + h_{im}^2}} \quad (26)$$

$$\text{OAE} = \frac{1}{N_{rg}} \sum_{i=1}^{N_{rg}} \frac{\text{area}(bbox_{g_i}) - \text{area}(bbox_{r_i})}{\text{area}(bbox_{g_i}) + \text{area}(bbox_{r_i})}. \quad (27)$$

The TRDR (Tracker Detection Rate) provides a general measure of the system's accuracy by describing the proportion of correct classifications for all frames in which ground truth is available. Similarly, the FAR (False Alarm Rate) determines how often the system claims an object is present when it is not.

Finally, the OTE (Object Tracking Error) quantifies the overall system error by measuring the average error of the tracked path with respect to ground truth for each object model. The equation has been modified from its original form by adding the $w_{im}^2 + h_{im}^2$ denominator. This normalises the pixel error (numerator) to the length of the image diagonal which represents the largest possible error. N_{rg} is the total number of ground truth points, (xg_i, yg_i) are the object's ground truth co-ordinates at frame i, and (xr_i, yr_i) is the object's classified position point. It should be noted that because the POD system does not take into account the 3-D pose information of the camera and scene, all co-ordinate measurements are in image space, i.e. x and y represent columns and rows in the image matrix.

An additional measurement which has been defined, owing to the 2-D nature of the system, is the Object Area Error (OAE). This is effectively the the average area difference between the bounding boxes of classified objects and their corresponding ground truth areas. N_{rg} is the total number of ground truth points, and $bbox_{g_i}$ and $bbox_{r_i}$ are the bounding boxes for the ground truth areas and classified objects respectively. Defining the area comparison in this way produces a measure in the range $(-1, 1)$ where a negative value indicates that the classified bounding boxes tend to be smaller than the ground truth, and a positive value the opposite.

7.1.2. Perceptual Complexity

In order to compare surveillance metrics between different types of video sequences a quantitative measurement is needed to relate the intrinsic differences between each sequence. A reasonable approach is to define the Perceptual Complexity (PC)

[4] A low importance corresponds to a low contribution of that object centre to the likelihood and visa versa.

for a sequence (suggested by [2]). The PC describes how 'difficult' a sequence is in the visual tracking sense. In this case, PC ratings are calculated for each test sequence based on a weighted combination of several quantities: the number and extent of occlusions; the similarity of colours between objects; and the overall image quality and variance.

7.1.3. Ground truth

Performance evaluation of vision system is largely dependent on the availability of ground truth data. Naturally, since real-time video has a data rate of between 25 and 30 frames per second, creating ground truth is exceedingly time consuming. Methods for obtaining ground truth range from using semi-automated tools [4] to estimation (eg. silhouette fitting [11]) and use of consistency measurements [5].

Fortunately, since the sequences used for evaluation are not excessively long, manual ground truth could be generated for each frame. The accuracy of the ground truth is not critical since the performance measurements only compare the bounding boxes.

7.2. Test Cases

The first test case is a short four person outdoor scene which was recorded with two Sony camcorders in an exterior environment. The second sequence consists of a single perspective security camera viewing a total of seven coloured people entering and walking around a room. Although the scene is indoors, there is a fair degree of variance close to the camera caused by the lighting arrangement, which causes certain people's shoulders to appear whiter when directly exposed. The final sequence used for testing comprises four ceiling-mounted cameras observing three people moving in a lab environment. This was created in an asynchronous manner by four different computers and the effect of a video network is simulated by processing the entire quartet of cameras iteratively in order of frame time stamps.

Tables 1 and 2 summarise scene information and overall results for the three test cases (processed on an Intel Pentium IV 2.8 GHz) respectively. Towards visualising the system performance, Figure 6 shows a labelled frame processed from Test Case 2. An example trajectory for Person 3 (green) is also shown as well as the overall confusion matrix for the whole test sequence.

Details	Case 1	Case 2	Case 3
Complexity (PC)	0.394	0.549	0.622
No. of cameras	2	1	4
No. of people	4	7	3
Running time (s)	30	90	200
Image resolution	360×240	384×288	285×189

Table 1: *Scene Information*

Performance Rating	Case 1	Case 2	Case 3
TRDR	0.89	0.85	0.76
FAR	0.025	0.00	0.03
OTE	0.15	0.16	0.24
OAE	-0.05	-0.18	-0.23
Processing rate	2.8 fps	1.8 fps	3.8 fps

Table 2: *Overall results*

The trajectory relates to the centres of the bounding boxes for the ground truth and matched areas respectively. The trajectory image also shows the actual matched positions by means of plotted triangles. The plotted trajectory is then constructed by using a 5-point moving average filter which removes spurious errors in the object's track. An idea of the tracking performance can be seen by comparing the matched trajectory to the ground truth path.

The improvement due to the incorporation of temporal information illustrates how the POD system could be used by other systems for recovery from failed tracking. As the POD system is designed to make instantaneous decisions about an object's location, it does not need to process every frame. Thus ideally, a fast time-dependent tracker could operate unencumbered and only use the POD at appropriate times (i.e. when its confidence is low). Since the primary objective of this work involves investigating the uses of colour in tracking, these applications have been left to future work.

7.3. Discussion

From the results, it is seen that the POD system is able to distinguish several people based only on colour information provided that there is enough variety in the trained models. There is a tendency for detected areas to be slightly smaller than the actual object (negative OAE trend). This has been attributed to the fact that lower object extremities are generally occluded by surrounding objects and shadows. This leads to the regions being filtered out either by the initial motion segmentation or the colour matching steps. The result is a smaller, raised bounding box.

The system proves to be robust through a number of differing camera environments and is not overly sensitive to parameter tuning. A beneficial aspect of the system is that it provides a realisable distributed framework which can be flexibly integrated with a variety of other systems. Its ability to make an instantaneous decision about any trained object allows it to cope with asynchronous video feeds and recovery from occlusions. By additional incorporation of temporal history, it has been shown in the presented test cases that a smooth trajectory can be extracted from a classified set at any time.

7.3.1. Overall Ratings

In order to assess the overall system performance, the results of each test case are compared, using their Perceptual Complexity (PC) as a relative basis. Figure 5 summarises the Tracker Detection Rates (TRDR) for the test cases.

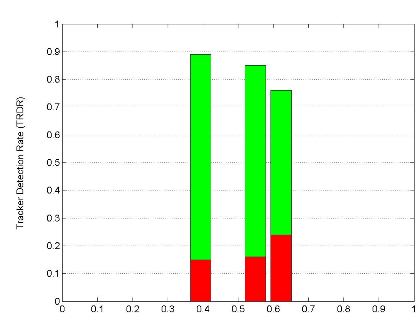

Figure 5: *Overall TRDR (upper green) and OTE (lower red) ratings for all test cases.*

As expected, the TRDR decreases as the PC increases. Unfortunately, without more test sets with high PC ratings, it is impossible to know the exact lower error bound of the system. Figure 5 also shows the average Object Tracking Error (OTE) for each sequence. The fact that the OTE seems to complement the TRDR confirms the fact that the TRDR is a truthful value. For instance, were a true positive hit acquired with a very large OTE, it would imply that the wrong object had accidently caused the detection rather than the actual one. Therefore this summarises the fact that, in general, the overall confusion between object classes is fairly low for the given test cases.

Finally, the False Alarm Rate (FAR) of the system is on average just below 2% with a mean processing rate of approximately 3 fps. The processing rate is not heavily affected by an increase in the number of trained objects. More elaborate optimisation of the current implementation could result in much faster frame rates.

7.3.2. *Colour Correction*

Quantifying the overall performance of the colour correction method is difficult, given the abstract nature of the process. Although comparative CIELAB values could be used to describe the improvements, this means very little when considering the system performance as a whole.

Based on the test cases (specifically Cases 1 and 3), there is approximately a 35% improvement when applying the method depending on the lighting characteristics of the scene.

7.3.3. *Colour difference metrics*

The 1976 CIELAB space was selected based on its perceptual uniformity. This property allows the Euclidean distance between points to be used as a colour difference metric. Unfortunately, further experiments have proved that CIELAB is not completely uniform [16] and does not provide a consistently good measure of the magnitude of perceptual difference between stimuli. This has lead to the definition of other, more optimised metrics such as CMC (British standard BS:6923), M&S (1980 Marks & Spencer equations for textile industry), BFD (refined CMC equations), and CIE 94 (simplified CMC version).

While it has not been proved whether any of these new metrics are better than the other, the British CMC equation, which uses user-configurable tolerance ellipsoids, is currently being considered as an ISO standard.

Since exact colour differences were not critical to the operation of the POD system (camera noise distorts image quality in any case), CIELAB, which is computationally simpler and more intuitive for spherical feature spaces, was retained.

7.3.4. *Online Adaptation*

It is important to note that while the POD system is able to adapt the colour models, this feature was not used for the test cases. Owing to the fact that the sequences are relatively short, it was thought that allowing adaptation would not significantly improve performance. Additionally, any improvement due to the adaptation would then mask the true performance of the matching process. Online adaptation has been dealt with extensively for Gaussian mixture models [9] and is known to improve long-term tracking. Thus the POD system can apply adaptation for situations in which there is more temporal variance.

8. Conclusions

A system capable of using the colour appearance of objects and people to detect their position within a digital video surveillance network has been presented. The system suggests a distributed, bottom-up implementation which can easily be integrated with off-the-shelf network products.

Features of the system include:

- Independence from camera pose and position
- Ability to deal with asynchronous video connections
- Persistence of object models over a distributed camera network
- Flexibility of integration with other visual tracking systems.

A bottom-up approach has been applied and each processing stage is fully modularised. Pre-processing consists of motion and colour segmentation, and a colour correction method for dealing with multiple views. System operation then proceeds in a two-stage process consisting of training and matching. Training involves representing objects as colour Gaussian mixtures which are then matched using a batch analytical method. While the implementation is equipped to perform online adaptation of the models, the test sequences are not very long. Thus it was thought that not using adaptation would provide a clearer view of the system's actual performance.

Some basic surveillance metrics have been applied in order to assess the performance of the system. An average accuracy of approximately 80% is achieved for overall system performance, though the exact performance is inversely proportional to the perceptual complexity of the scene. The system exhibits a very low false alarm rate and is capable of an average processing rate of 3 fps with little dependence on the number of tracked objects. It is envisaged that further work may yield better optimisation with faster frame rates.

9. Future work

While current 3-D tracking systems obtain good results, a common weakness is their inability to recover from failure. Since the POD system is able to generate a hypothesis without being dependent on temporal priors, it is thought that the combination of the system with a 3-D tracker could produce a viable solution. One possibility is for the 3-D tracker to exploit the POD's ability to deal with asynchronous video by only presenting it with frames when the overall system confidence is low. Alternatively, the POD could be used full-time for providing a Kalman or particle filter with observations.

While the system can be applied to assisting real-time tracking systems, it is also thought that the ideas presented may hold further application in automated image retrieval and robotic vision areas. It is hoped that further extension of this work combined with robust 3-D tracking systems such as [10] could lead to an eventual real-time solution.

10. Acknowledgements

Many thanks to TSS Technology, De Beers and the National Research Foundation for supporting this research. Additional thanks go to Markus Louw who hand-segmented ground truth for the test sequences.

11. References

[1] H. Austermeier, G. Hartmann, and R. Hilker. Color-calibration of a robot vision system using self-organizing feature maps. *ICANN*, pages 257–262, 1996.

[2] J. Black, T. Ellis, and P. Rosin. A novel method for video tracking performance evaluation. In *Joint IEEE International Workshop on VS-PETS*, October 2003.

[3] P. J. Burt, T. H. Hong, and A. Rosenfeld. Segmentation and estimation of image region properties through cooperative hierarchical computation. *IEEE Transactions On Systems, Man, and Cybernetics*, 11(12):802–809, 1981.

[4] D. Doermann and D. Mihalcik. Tools and techniques for video performance evaluation. In *Proceedings of the Third International Workshop on PETS*, June 2002.

[5] C. Erdem, B. Sankur, and A. M. Tekalp. Metrics for performance evaluation of video object segmentation and tracking without ground-truth. In *IEEE International Conference on Image Processing*, October 2001.

[6] I. Haritaoglu, D. Beymer, and M. Flickner. Video-CRM: Detection and tracking people in stores. In *Joint IEEE International Workshop on VS-PETS*, October 2003.

[7] Intel. *Open Source Computer Vision Library Reference Manual*. Intel Corporation, USA, 2001. [Online]. Available: http://www.sourceforge.net/projects/opencvlibrary/index.html [February 2004].

[8] A. Kosir and J. F. Tasic. Pyramid segmentation parameters estimation based on image total variation. In *Proceedings of IEEE conference EUROCON 2003*, 2003.

[9] S. J. McKenna, Y. Raja, and S. Gong. Tracking colour objects using adaptive mixture models. *Image Vision Computing*, 17:225–231, 1999.

[10] B. Merven, F. Nicolls, and G. de Jager. Multi-camera person tracking using an extended kalman filter. In *Fifteenth Annual Symposium of the Pattern Recognition Association of South Africa*, 2003.

[11] A. Senior. Real-time articulate human body tracking using silhouette information. In *Joint IEEE International Workshop on VS-PETS*, October 2003.

[12] P. Y. Simard, L. Bottou, P. Haffner, and Y. L. Cun. Boxlets: a fast convolution algorithm for signal processing and neural networks. In *Advances in Neural Information Processing Systems*, volume 11, pages 571–577. 1999.

[13] S. W. Smith. *The Scientist and Engineer's Guide to Digital Signal Processing*. California Technical Publishing, 1997.

[14] C. Stauffer and W. Grimson. Adaptive background mixture models for real-time tracking. In *Computer Vision and Pattern Recognition*, 1999.

[15] P. Viola and M. Jones. Robust real-time object detection. In *Second International Workshop on Statistical and Computational Theories of Vision — Modeling, Learning, Computing, and Sampling*, 2001.

[16] S. Westland. Frequently asked questions about colour physics. Technical report, Colourware, 2000. [Online]. Available: http://www.colourware.co.uk/cpfaq.htm [January 2004].

[17] G. Wyszecky and W. S. Stiles. *Color Science: Concepts and Methods, Quantitative Data and Formulas*. J. Wiley & Sons, New York, 1982.

(a) Example matched frame

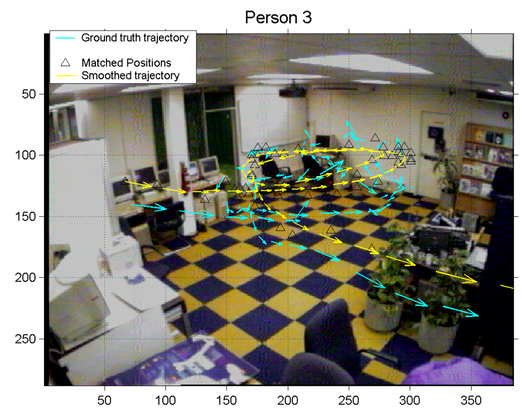

(b) Overall trajectory for Person 3 (green)

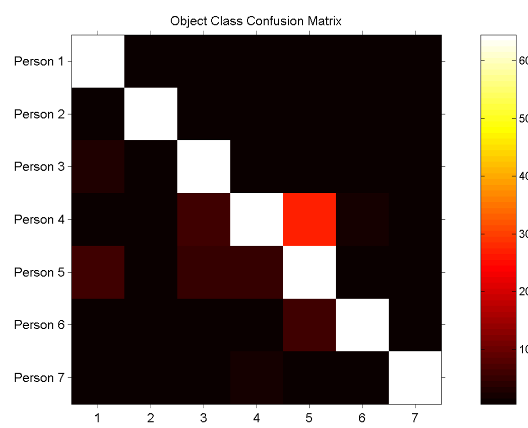

(c) Overall Confusion Matrix

Figure 6: *Example result images taken from Test Case 2.*